

Probabilistic Slope Stability Analysis using RFEM with Non-Stationary Random Fields

D.V. GRIFFITHS^{a,b}, J. HUANG^b and G.A. FENTON^c

^a Dept of Civil and Environmental Engineering, Colorado School of Mines, USA,

^b Center for Geotechnical Science and Engineering, University of Newcastle, Australia

^c Dept of Engineering Mathematics and Internetworking, Dalhousie University, Canada

Abstract. Using recently obtained deterministic results as a benchmark, probabilistic slope stability analyses have been performed on an undrained slope using the random finite element method (RFEM). Non-stationary random fields have been generated with linearly increasing mean undrained strength and a constant coefficient of variation. The influence of input spatial correlation and variance on the probability of slope failure in a test example is reported, and particular attention is drawn to the solutions corresponding to extreme values of the spatial correlation length.

Keywords. slope stability, finite elements, RFEM, random fields

1. Introduction

In the world of probabilistic geotechnical analysis, it seems likely that slope stability analysis has received more attention than any other application. A very significant bibliography is now available which is too extensive to mention here, but important early contributions in the 1970s include those of Matsuo and Kuroda (1974), Alonso (1976), Tang et al. (1976) and Vanmarcke (1977). Research from the University of New South Wales group deserves special mention including that of Mostyn and Li (1993) from which the title of this session, namely “Probabilistic Slope Stability Analysis: The State of Play” was borrowed. Recognition of the importance that statistical approaches might play in geotechnical analysis goes back much further. In his foreword to the inaugural issue of the journal *Géotechnique* in 1948, Karl Terzaghi talked about soil properties varying “...*from point to point.*” Probabilistic tools have subsequently been developed ranging from event trees to first order reliability and moment methods (e.g. Whitman 1984, Wolff 1996, Lacasse 1994, Christian et al. 1994, Hassan and Wolff 2000, Duncan 2000).

It is only quite recently however, that Terzaghi’s observation of spatially varying soil

properties has been tackled explicitly by the Random Finite Element Method (RFEM). In the work of Griffiths and Fenton (2000, 2004), slope stability analyses were presented using elastic-plastic RFEM. The random fields were generated using the Local Averaging Subdivision (LAS) method (Fenton and Vanmarcke 1990) which is able to model spatial variability while properly accounting for local averaging over each finite element. The deliverable in such an analysis by RFEM is the *probability of failure* as opposed to the classical *factor of safety*. Several papers written by the authors have used RFEM to considered slopes with stationary random properties, however this paper will describe some probabilistic analyses of undrained slopes with non-stationary random fields, in which the mean and standard deviation of soil strength increase linearly with depth.

The general slope geometry and parameters as used in this study are shown in Figure 1 together with a typical finite element mesh.

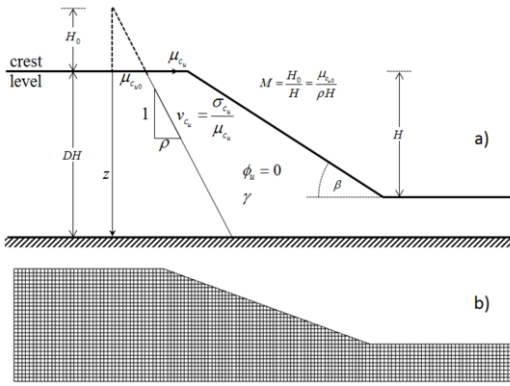


Figure 1. a) Slope geometry and soil properties b) typical finite element mesh.

Figure 1a shows that the mean undrained strength is a linear function of depth according to the equation

$$\mu_{c_{iz}} = \mu_{c_{i0}} + \rho z \tag{1}$$

where $\mu_{c_{iz}}$ is the mean strength at depth z , $\mu_{c_{i0}}$ is the mean strength at crest level and ρ is the gradient of mean strength. In this study the standard deviation of undrained strength is also assumed to be a linear function of depth with a gradient that results in a constant coefficient of variation v_{c_u} . It can also be noted that the spatial correlation length θ is assumed to be constant and isotropic in this study. Other parameters include the undrained friction angle $\phi_u = 0$ and the saturated unit weight γ . The slope is inclined to the horizontal at angle β , with height H and depth ratio to a lower firm layer D .

2. Random Field Generation with Linearly Increasing Mean Strength

The random field generation is based on the RFEM method which is described in detail in Fenton and Griffiths (2008). Full source code RFEM downloads are available at the web site www.mines.edu/~vgriffit/rfem

Initially, a homogeneous, stationary, lognormal random field based on the parameters at $z = 0$, i.e. mean $\mu_{c_{i0}}$, standard deviation $\sigma_{c_{i0}}$ and spatial correlation length θ is generated across the mesh. The element values are then scaled to account for depth $z > 0$ using

$$c_z = c_0 \frac{\mu_{c_{i0}} + \rho z}{\mu_{c_{i0}}} \tag{2}$$

Eq. (2) shows that a quite simple adjustment to c_0 from the initial stationary random field is needed to deliver the non-stationary c_z with linearly increasing mean strength and constant coefficient of variation..

An example of some typical simulations are shown in Fig.2, for a relatively short spatial correlation of $\theta = 3m$

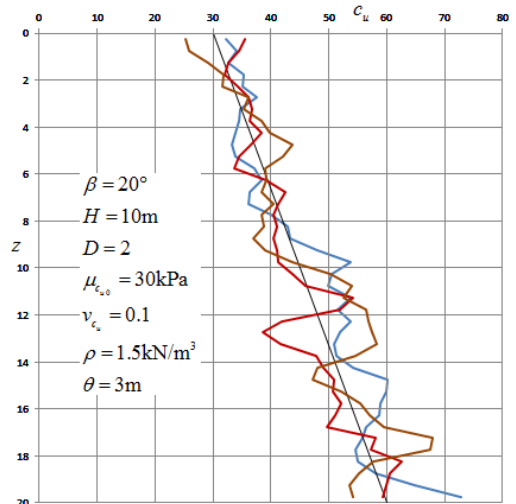


Figure 2. Three typical simulations of a linearly increasing random field ($\theta = 3m$)

Higher spatial correlation lengths will lead to smoother variations with depth, and for a typical simulation, few crossings of the linearly increasing mean line.

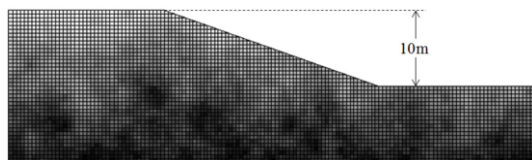


Figure 3. Grey-scale representation of a simulated random field with linearly increasing strength with depth ($\theta = 10\text{m}$). Dark is stronger, light is weaker.

3. Probabilistic Slope Stability by RFEM

Following generation of the non-stationary random field as described above, a finite element slope stability analysis is performed. The finite element code is run in a “Fail/No-Fail” mode (e.g. Griffiths and Fenton 2004) where each simulation of the Monte-Carlo process results in a binary result depending on whether the algorithm converges within 500 iterations (no fail), or hits the iteration ceiling of 500 (fail). Although 500 is user- defined and other values could be used, it has been determined that simulations needing ≥ 500 iterations clearly indicate the population of failed slopes. After a sufficient number of simulations have been performed, the probability of failure p_f is simply the number of simulations that indicate failure, divided by the total number of simulations.

4. Number of Monte-Carlo Simulations

The number of Monte-Carlo simulations needed to obtain stable output is largely a function of the variability of the input. Figure 4 shows the probability of failure as a function of the number of simulations for a typical slope example. Reasonably stable and reproducible results are seen to occur when the number of simulations reaches $n_{sim} = 1000$.

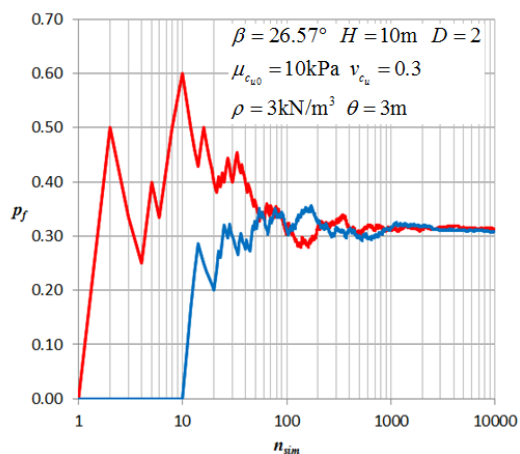


Figure 4. Check on the number of Monte-Carlo simulations needed for statistical stability.

5. Results of Probabilistic Slope Analysis

A comprehensive set of analyses and parametric studies have been performed on the probabilistic slope stability problem with linearly increasing mean strength. In the current paper, a slope with the geometry and properties given in Table 1 will be considered.

Table 1. Geometry and properties of test slope

β	20°
H	10 m
D	1.5
$\mu_{c_{u0}}$	18 kPa
ρ	2.4 kN/m^3
γ	20 kN/m^3

Based on the work of Hunter and Schuster (1968), and the more recent refinements of Griffiths and Yu (2015), a deterministic analysis of the slope indicated in Table 1 would have a factor of safety of $FS = 1.51$, with a critical failure circle tangent to a depth ratio of $D = 1.38$. It may be noted that the deterministic critical failure mechanism does not go to the full depth of $D = 1.5$, as would be the case for a $\beta = 20^\circ$ slope if c_u was constant.

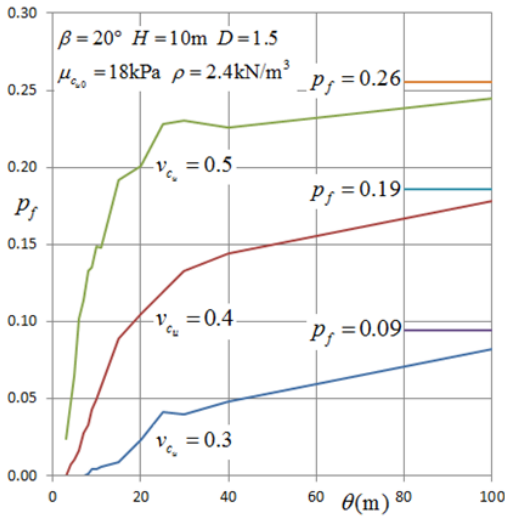


Figure 5. Probability of slope failure as a function of spatial correlation length and coefficient of variation.

The computed probability of failure by RFEM for a range spatial correlation lengths and coefficients of variation is given in Fig.5.

The results show that the probability of failure p_f increases with both the coefficient of variation v_{c_u} and the spatial correlation length θ .

In this particular example, the highest probability of failure corresponds to the highest spatial correlation lengths. This is not always the case in probabilistic slope stability analysis however, where steeper slopes with stationary random fields can sometimes indicate a “worst case” spatial correlation length of the order of the slope height ($\theta \approx H$) (see e.g. Allahverdizadeh 2015). It is expected that slopes with linearly increasing strength may also exhibit this “worst case” phenomenon, which will be explored as part of a much broader parametric study.

Returning to the results of the example problem presented in Fig.5, insight into the role of spatial correlation on the probability of failure can be obtained by considering the limiting cases of very small ($\theta \rightarrow 0$) and very large ($\theta \rightarrow \infty$) spatial correlation lengths (e.g. Griffiths et al. 2009).

5.1. Very Small Spatial Correlation Length

As $\theta \rightarrow 0$, $\mu_{c_u} \rightarrow \text{Median}_{c_u}$ and $\sigma_{c_u} \rightarrow 0$ for all z due to local averaging of a lognormal process. Each Monte-Carlo simulation is therefore essentially identical and deterministic, with an adjusted linear strength profile given by

$$c_{uz} = \frac{\mu_{c_{u0}}}{(1 + v_{c_u}^2)^{1/2}} + \frac{\rho}{(1 + v_{c_u}^2)^{1/2}} z \quad (3)$$

Typical values of the adjusted surface value at $z = 0$ and strength gradient from Eq.(3) are given in Table 2.

Table 2. Deterministic linear strength parameters from Eq.(3) for the slope from Table 1 as $\theta \rightarrow 0$

v_{c_u}	$\frac{\mu_{c_{u0}}}{(1 + v_{c_u}^2)^{1/2}}$ (kPa)	$\frac{\rho}{(1 + v_{c_u}^2)^{1/2}}$ (kN/m ³)	FS	p_f
0.0	18.00	2.40	1.51	0
0.3	17.24	2.30	1.45	0
0.4	16.71	2.23	1.41	0
0.5	16.10	2.15	1.35	0
0.7	14.75	1.97	1.24	0
0.9	13.38	1.78	1.13	0
1.1	12.11	1.61	1.02	0
1.14	11.89	1.59	1.00	1
1.3	10.97	1.46	0.92	1

It is seen from Table 2 that as the input coefficient of variation is increased, the surface strength and gradient are proportionately reduced. For the cases considered in Fig.5, namely $v_{c_u} = 0.3, 0.4, 0.5$ as highlighted in the table, the deterministic factor of safety is always greater than unity, hence $p_f \rightarrow 0$. It can also be noted from the table however, that as v_{c_u} is further increased, the deterministic factor of safety eventually becomes less than unity and $p_f \rightarrow 1$. The sudden switch from $p_f \rightarrow 0$ to $p_f \rightarrow 1$ occurs at about $v_{c_u} = 1.14$ which would be considered a high variability, even for an undrained strength (e.g. Lee et al. 1983). It may be noted from Eq.(3) that the extrapolated

strength profiles corresponding to different v_{c_u} values all pass through the same point above the crest at a height given by

$$z_0 = -\frac{\mu_{c_u}}{\rho} \tag{4}$$

For the particular slope under consideration the common point is at $z_0 = -7.5\text{m}$ as shown in Fig.6.

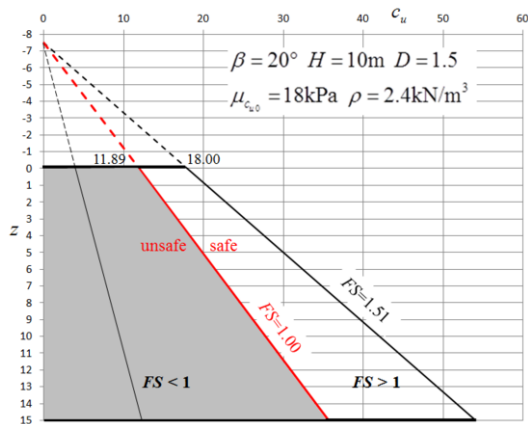


Figure 6. Linear undrained strength distributions showing transition from safe to unsafe conditions.

5.2. Very Large Spatial Correlation Length

As $\theta \rightarrow \infty$, each Monte-Carlo simulation gives a linearly increasing strength profile, but all different to each other. Based on Eq.(2) it can be shown that each simulation has a strength profile given by

$$c_{uz} = c_{u0} + \left(\frac{\rho c_{u0}}{\mu_{c_{u0}}} \right) z \tag{5}$$

where c_{u0} is randomly picked from a lognormal distribution with mean $\mu_{c_{u0}}$ and coefficient of variation v_{c_u} . As with Eq.(3), the extrapolated strength distributions all pass through the same point as given by Eq.(4).

As shown in Fig. 6 and Table 2, slope failure occurs when $c_{u0} < 11.89\text{kPa}$. Since c_{u0} is lognormally distributed with a mean of

$\mu_{c_{u0}} = 18\text{kPa}$ the probability of failure p_f will depend on v_{c_u} .

Take for example, the case in Fig.5 where $v_{c_u} = 0.5$. The mean and standard deviation of the underlying normal distribution of $\ln c_{u0}$ are given from standard transformations as

$$\sigma_{\ln c_{u0}} = \sqrt{\ln\{1 + 0.5^2\}} = 0.4724 \tag{6}$$

$$\mu_{\ln c_{u0}} = \ln(18) - \frac{1}{2} \times 0.4724^2 = 2.7788$$

The probability of failure is therefore given by

$$\begin{aligned} p_f &= 1 - \Phi\left(\frac{2.7788 - \ln(11.89)}{0.4724}\right) \\ &= 1 - \Phi(0.6416) \\ &= 0.26 \text{ (26\%)} \end{aligned} \tag{7}$$

where Φ is the cumulative distribution function. Similar operation for the cases where $v_{c_u} = 0.4$ and $v_{c_u} = 0.3$ lead to $p_f = 0.19$ and $p_f = 0.09$ respectively, which define the asymptotic values the results are approaching in Fig.5 as $\theta \rightarrow \infty$.

6. Concluding Remarks

The paper has described probabilistic analysis of an undrained slope with linearly increasing mean strength and constant coefficient of variation. In the example presented, the probability of failure increased monotonically with the coefficient of variation and the spatial correlation length of undrained strength. Attention was also drawn to probabilistic behavior corresponding to extreme values of the spatial correlation length where $\theta \rightarrow 0$ and $\theta \rightarrow \infty$ enabling validation against deterministic values. Results presented in this paper form a subset of a much larger probabilistic study on undrained slopes with linearly increasing strength, which will be reported elsewhere.

References

- Allahverdizadeh, P. (2015). Risk assessment and spatial variability in geotechnical stability problems, *PhD Thesis*, Colorado School of Mines, Golden, USA.
- Alonso, E.E. (1976). Risk analysis of slopes and its application to slopes in Canadian sensitive clays, *Géotechnique*, vol.26, pp.453-472.
- Christian, J.T., Ladd, C.C., Baecher, G.B. (1994) Reliability applied to slope stability analysis, *J Geotech Eng, ASCE*, vol.120, no.12, pp.2180-2207.
- Duncan, J.M. (2000). Factors of safety and reliability in geotechnical engineering, *J Geotech Geoenv Eng*, vol.126, no.4, pp.307-316.
- Fenton G.A., Vanmarcke, E.H., (1990). Simulation of random fields via local average subdivision, *J Eng Mech*, vol.116, no.8, pp. 1733-1749.
- Fenton G.A., Griffiths, D.V. (2008). *Risk Assessment in Geotechnical Engineering*, John Wiley & Sons, Hoboken, NJ.
- Griffiths, D.V., Fenton G.A. (2000) Influence of soil strength spatial variability on the stability of an undrained clay slope by finite elements, *Proceeding of GeoDenver 2000, Slope Stability 2000*, Griffiths, D.V. et al (eds.), pub. ASCE, GSP 101, pp.184-193.
- Griffiths, D.V., Fenton G.A. (2004). Probabilistic slope stability analysis by finite elements, *J Geotech Geoenv Eng*, vol.130, no.5, pp. 507-518.
- Griffiths, D.V., Huang, J., Fenton, G.A. (2009). Influence of spatial variability on slope reliability using 2-D random fields, *J Geotech Geoenv Eng*, vol.135, no.10, pp. 1367-1378.
- Griffiths, D.V., Yu, X. (2015). Another look at the stability of slopes with linearly increasing undrained strength. Under review.
- Hassan, A.M., Wolff, T.F. (2000) Effect of deterministic and probabilistic models on slope reliability index, *Proceeding of GeoDenver 2000, Slope Stability 2000*, Griffiths, D.V. et al (eds.), pub. ASCE, GSP 101, pp.194-208.
- Hunter, J.H., Schuster, R.L. (1968). Stability of simple cuttings in normally consolidated clay. *Géotechnique*, Vol.18, No.3, pp.372-378.
- Lacasse, S. (1994) Reliability and probabilistic methods, *Proceedings 13th ICSMFE*, New Delhi, India, pp.225-227.
- Lee, I. K., White, W., Ingles, O. G. (1983). *Geotechnical Engineering*, pub. Pitman, London.
- Matsuo, M., Kuroda, K., (1974). Probabilistic approach to the design of embankments. *Soils and Foundations*, vol.14, no.1, pp.1-17.
- Mostyn, G.R., Li, K.S. (1993). Probabilistic slope stability - State of play., *Proceedings Conf Probabilistic Meths Geotech Eng*, Li, K.S. and Lo, S-C.R. (eds.), Pub. A.A. Balkema, pp.89-110.
- Tang, W.H., Yucemen, M.S., Ang, A.H.S. (1976). Probability based short-term design of slopes, *Can Geotech J*, vol.13, pp.201-215.
- Vanmarcke, E.H. (1977). Reliability of earth slopes, *J Geotech Eng, ASCE*, vol.103, no.11, pp.1247-1265.
- Whitman, R.V. (2000). Organizing and evaluating uncertainty in geotechnical engineering, *J Geotech Geoenv Eng*, vol.126, no.7, pp.583-593.
- Wolff, T.F. (1996) Probabilistic slope stability in theory and practice, *Proceedings, Uncertainty in the geologic environment: From theory to practice*, C.D. Shackelford et al. (eds.), Madison, WI, pub. ASCE, GSP 58, vol.2, pp. 419-433.